areas as determined from UPD. This may reflect the presence of pinholes which add to the exposed surface but are not sufficiently large to permit ZnTPP incorporation. This possibility may be tested by two different methods. The first is an independent measurement of the amount of adsorbate in a reconstituted system using an electroactive adsorbate. The second involves the use of *n*-octadecyl mercaptan (OM) to block pinhole sites.

In conclusion, the results presented herein demonstrate the considerable selectivity provided by self-assembled monolayers. A series of porphyrins of similar size and shape were readily reconstituted in sites prepared from ZnTPP. On the other hand, MgPC and BChl, which differ only in the substituents on the periphery of the macrocycle, were not reincorporated. The quantitative estimates of ZnTPP by SERRS were found to be somewhat lower than the surface area measurements provided by UPD. The difference is probably due to the presence of pinholes in the OTS/template system. The total area of the OTS matrix and template system appears measurably below the ideal 100% value; for the purposes of construction of molecular-recognizing template sites, it would appear that the small void volume always present is not an impediment to the efficiency of the formation of systems having a high degree of species specificity.

Acknowledgment. The financial support of the U.S. Department of Energy, Chemical Sciences Division (DE-FG02-84ER13261), is gratefully acknowledged.

Photochemistry of O_3/HNCO Mixtures

A. P. Ongstad, X. Liu, and R. D. Coombe*

Department of Chemistry, University of Denver, Denver, Colorado 80208 *(Received: June 6, 1988; In Final Form: July 25, 1988)*

Pulsed photolysis of gaseous O_3/HNCO mixtures at 249 nm produces emission from the NH $A^3\Pi \rightarrow X^3\Sigma^-$ transition near 336 nm. The data suggest that the excited NH is produced by the reaction $O(^1D) + HNCO \rightarrow NH + CO_2$. The branching fraction to the alternate products OH + NCO is less than 0.1. This mechanism is quite different from that of the analogous $O(^1D) + HN_3$, $NH(^1\Delta) + HN_3$, and $NH(^1\Delta)$ + HNCO reactions. From the time profile of the NH emission, the rate constant for $O(^1D)$ + HNCO is determined to be $(4.6 \pm 0.4) \times 10^{-11}$ cm^3 s^{-1}.

Introduction

In a recent study[1] of the photolysis of O_3/HN_3 mixtures, it was shown that the reaction of $O(^1D)$ atoms with HN_3 is rapid and produces OH + N_3. This behavior is similar to that of the isoelectronic $NH(a^1\Delta)$ reaction with HN_3,[2] which produces NH_2 + N_3. The reaction of $O(^1D)$ atoms with N_3 radicals occurs subsequent to $O(^1D) + HN_3$ and produces chemiluminescence from the $A^2\Sigma^+ \rightarrow X^2\Pi$ transition in NO. The temporal profile of this emission was modeled to obtain rate constants for the $O(^1D)$ + HN_3 and $O(^1D)$ + N_3 elementary reactions.

In this paper, we describe similar observations of the reaction between $O(^1D)$ and HNCO. The analogous $NH(a^1\Delta)$ + HNCO reaction has been studied from HNCO photolysis[3,4] and is thought to produce NH_2 + NCO. The rate constant for $NH(a^1\Delta)$ + HNCO has been reported to be 1.45×10^{-10} cm^3 s^{-1} by Drozdoski and co-workers.[3] The results of the present experiments indicate that $O(^1D)$ + HNCO proceeds by a route entirely different from that found for either the $O(^1D) + HN_3$ reaction or the $NH(a^1\Delta)$ reactions noted above.

Experimental Section

The methods employed were similar to those described in ref 1. O_3 (about 65% purity, the remainder being O_2) was prepared with a commercial ozonizer and stored in a Pyrex flask. HNCO was generated by heating mixtures of KOCN and excess stearic acid to 373 K and collecting the gaseous product in a Pyrex flask. The gaseous HNCO was diluted to a 10% mixture with helium. FTIR analysis indicated no apparent impurities in the gas mixture. Slow flows of O_3 and HNCO were mixed upstream of a photolysis cell, which was 20 cm in length and fabricated from stainless steel. The total pressure in the cell was measured with a capacitance manometer. The partial pressure of O_3 in the cell was measured by optical absorption at 253.7 nm. There was no evidence of prereaction between the flowing O_3 and HNCO.

The gas mixtures were photolyzed with the 249-nm output of a pulsed excimer laser. Chemiluminescence produced by the photolysis was detected with a 0.25-m monochromator and cooled GaAs photomultiplier tube. The presence of nonemitting species was probed by recording laser-induced fluorescence (LIF) excitation spectra. A nitrogen laser pumped dye laser (PRA LN107) was used as a probe in the LIF experiments. Spectra were recorded with a gated boxcar integrator interfaced to a microcomputer. Time profiles of the emission were recorded with a Nicolet 1270 pulsed data collection system which also was interfaced to a microcomputer. Analysis of the data was performed with an RS/1 statistical package on a VAX 780 mainframe computer.

Results and Discussion

Since the absorption cross section of O_3 is very large[5] and that of HNCO[6] is very small at 249 nm, photolysis at this wavelength selectively dissociates the O_3. Excited $O(^1D)$ and $O_2(a^1\Delta)$ are produced in 90% yield.[7] To the extent that this system is similar to O_3/HN_3, the $O(^1D)$ would react with HNCO to produce OH + NCO and then with NCO to produce excited NO and CO. The latter reaction (O^1D + NCO) is exothermic by 148 kcal mol^{-1}, easily sufficient to produce $NO(A^2\Sigma^+)$. Figure 1 shows a portion of the UV chemiluminescence recorded subsequent to photolysis at 249 nm. There is no detectable emission from the $A \rightarrow X$ transition in NO. Instead, the spectrum is dominated by emission from the $A^3\Pi \rightarrow X^3\Sigma^-$ transition in NH near 336 nm. Very much less intense emission from the $A^2\Sigma^+ \rightarrow X^2\Pi$ transition in OH was found when the maximum amplifier gain of the detection system was employed. Although these transitions in NH and OH were also observed[1] from photolysis of O_3/HN_3, they were more than

(1) Ongstad, A. P.; Coombe, R. D.; Neumann, D. K.; Stech, D. J. *J. Phys. Chem.*, in press.
(2) McDonald, J. R.; Miller, R. G.; Baronavski, A. P. *Chem. Phys.* **1978**, *30*, 133.
(3) Drozdoski, W. S.; Baronavski, A. P.; McDonald, J. R. *Chem. Phys. Lett.* **1979**, *64*, 421.
(4) Spiglanin, T. A.; Perry, R. A.; Chandler, D. W. *J. Phys. Chem.* **1986**, *90*, 6184.
(5) Braun, W.; et al. *J. Phys. Chem. Ref. Data* **1973**, *2*, 267.
(6) Rabalais, J. W.; McDonald, J. R.; McGlynn, S. P. *J. Chem. Phys.* **1969**, *51*, 5103.
(7) Brock, J. C.; Watson, R. T. *Chem. Phys. Lett.* **1980**, *71*, 371.

0022-3654/88/2092-5578$01.50/0

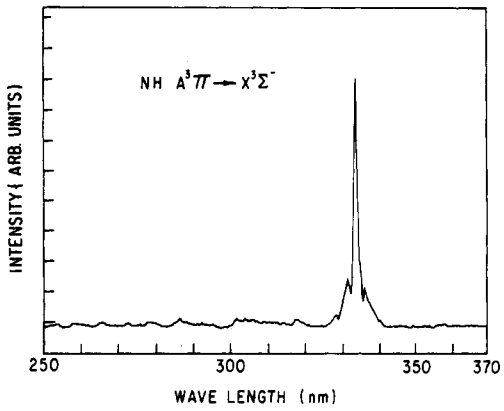

Figure 1. A portion of the UV emission spectrum recorded from 249-nm photolysis of an O_3/HNCO mixture.

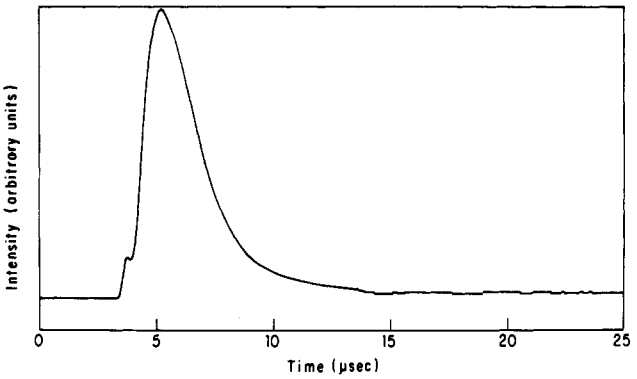

Figure 2. A typical time profile of the NH A → X emission, recorded for the 0,0 band near 336 nm. For the data shown, [HNCO] = 5.2×10^{15} cm^{-3}, $[O_3]_0 = 1.2 \times 10^{15}$ cm^{-3}, and $[O(^1D)]_0 = 4.8 \times 10^{14}$ cm^{-3}.

2 orders of magnitude weaker than the NO A → X emission in that system, and the OH transition was nearly as intense as the NH transition.

A representative time profile of the NH emission from O_3/HNCO is shown in Figure 2. The profile exhibits a risetime of less than 1 μs and a decay extending for several microseconds. The rise of the emission corresponds to the rate of decay of the excited NH, a convolution of the radiative lifetime[8] of the $A^3\Pi$ state (455 ns) with the time constant of the detection electronics (400 ns, limited by an amplifier). The decay of the emission corresponds to the rate of collisional formation of the excited NH. This rate was observed to vary with the excess density of HNCO, for a fixed initial O_3 density. The individual decays were found to be exponential over a wide range of HNCO densities. Figure 3 shows a plot of the exponential decay rate vs the HNCO density. From the slope of the plot, the apparent second-order rate constant for NH(A) production is $(4.6 \pm 0.4) \times 10^{-11}$ cm^3 s^{-1}. The plot shows a large intercept at zero HNCO density, corresponding to the rate of $O(^1D)$ loss in the absence of HNCO. Assuming that quenching by residual O_3 dominates this loss (only about 45% of the initial O_3 present was dissociated by a typical laser pulse), the rate constant for the $O(^1D) + O_3$ reaction is calculated to be $(3.0 \pm 0.2) \times 10^{-10}$ cm^3 s^{-1} from the intercept. This value is in good agreement with direct measurements of the $O(^1D) + O_3$ rate reported in the literature.[7,9]

The intensity of the NH emission was unaffected by large changes in the HNCO density but was significantly enhanced by small increases in the O_3 density. To quantify this relationship, the dependence of the time-integrated emission intensity on the initial $O(^1D)$ density was measured. The $O(^1D)$ density was varied by changing the incident laser fluence for a fixed initial O_3 density. The fluence was varied from 0.07 to 0.5 mJ cm^{-2}. Initial $O(^1D)$ densities in front of the observation port were calculated from the following expression:[10]

$$[O(^1D)] = 0.9[O_3]_0\{1 - [1 + e^{-z/d}(e^{\sigma\phi} - 1)]^{-1}\}$$

where σ is the absorption cross section[5] of O_3 at 249 nm, d is the optical depth, and ϕ is the time-integrated photon flux in photons cm^{-2}. For the geometry of this apparatus, the photolysis depth (z) was 10 cm. Since the data described above indicate that the rate constant for $O(^1D)$ reaction with HNCO is nearly an order of magnitude smaller than that for its reaction with O_3, a significant fraction of the initial $O(^1D)$ present is removed by O_3, even for large excess HNCO densities. Hence, the integrated NH A → X intensities were corrected for this fraction, which varied inversely with the incident laser fluence. Figure 4 shows a log–log plot of the corrected intensity vs the initial $O(^1D)$ density. The slope of the plot is 1.03 ± 0.02, indicating a linear relationship between the excited NH(A) and $O(^1D)$.

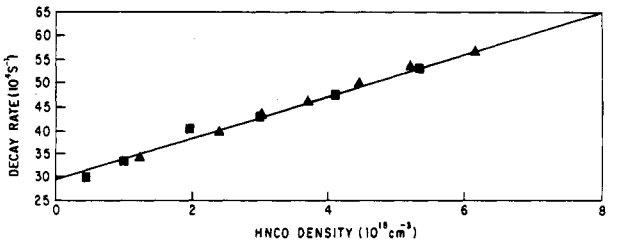

Figure 3. First-order decay rate of the NH A → X emission intensity vs the density of HNCO. Squares and triangles represent data from two different sets of experiments. The initial $O(^1D)$ density was near 5×10^{14} cm^{-3}.

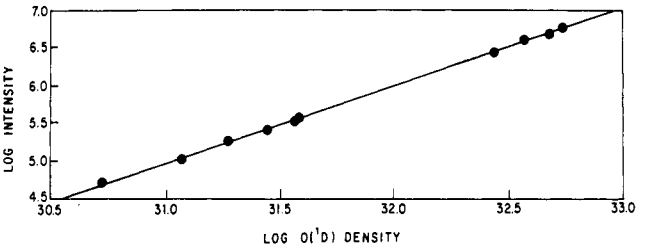

Figure 4. log of the NH A → X emission intensity vs log of the initial $O(^1D)$ density. A linear least-squares fit to the plot has a slope of 1.03 ± 0.02.

The presence of NCO radicals in the reaction medium was probed by LIF on the $X^2\Pi \rightarrow A^2\Sigma^+$ transition of this molecule near 438 nm. The probe pulse was timed to pass through the medium approximately 3 μs after the 249-nm photolysis pulse, i.e., after the large majority of the $O(^1D)$ atoms were removed by reaction with HNCO or O_3. LIF experiments were performed over a broad range of O_3 and HNCO densities, up to 3.2×10^{15} and 5.6×10^{14} cm^{-3}, respectively. NCO was not detected in any of these experiments.

These results are in strong contrast to those found for the O_3/HN_3 system.[1] In that case, NO(A) was the dominant emitter, and its intensity varied quadratically with the initial $O(^1D)$ density in accord with the two-step formation sequence noted above. Further, the rate constant of the $O(^1D) + HN_3$ reaction was found to be 3.2×10^{-10} cm^3 s^{-1}, similar to the large rate constants reported[2,3] for $NH(a^1\Delta)$ reactions with HN_3 and HNCO. From the spectra of chemiluminescence from the O_3/HNCO system, the time profile of the NH A → X emission, and the linear relationship between intensity and $O(^1D)$ density, we propose that the primary reaction in this system is

$$O(^1D) + HNCO \rightarrow NH + CO_2 \qquad \Delta H = -92 \text{ kcal mol}^{-1} \tag{2}$$

This process involves direct attack of the excited oxygen atom on the carbon atom of the NCO linkage, rather than abstraction of

(8) Smith, W. H.; Brzozowski, J.; Erman, P. *J. Chem. Phys.* **1976**, *64*, 4628.

(9) Amimoto, S. T.; Force, A. P.; Wiesenfeld, J. R. *Chem. Phys. Lett.* **1978**, *60*, 40.

(10) Bellman, R.; Birnbaum, G.; Wagner, W. G. *J. Appl. Phys.* **1963**, *34*, 780.

the hydrogen atom as occurs in $O(^1D) + HN_3$. Since production of NH(A) as observed in these experiments is exothermic by only 7 kcal mol^{-1}, the branching fraction to this excited state is likely to be small. Indeed, spin conservation would predict the formation of excited singlet states of NH (i.e., $a^1\Delta$ or $b^1\Sigma^+$) in reaction 2. It is not surprising that emission from these states was not observed in our experiments, given their very long radiative lifetimes.[11]

The absence of NCO radicals in the reaction medium argues that process 2 above is the dominant route for $O(^1D)$ reaction with HNCO. In order to quantify this result, experiments were performed to determine the detection limit of the NCO LIF experiments. For this purpose, NCO radicals were produced by admission of a known flow of HNCO to excess F atoms (from a discharge through CF_4/Ar) in a discharge-flow assembly which was affixed to the photolysis cell. This reaction[12] rapidly produces HF + NCO, and LIF from the NCO radicals was readily detected. Assuming that HNCO is converted to NCO with unit efficiency, the minimum density of NCO detectable by the LIF experiment was determined to be $<2 \times 10^{12}$ cm^{-3} from the signal-to-noise ratio of the experiment. This value may be compared with the density of $O(^1D)$ atoms that undergo reaction with HNCO in the O_3/HNCO photolysis experiments (where no NCO was detected), which can be calculated from the initial $O(^1D)$ density, the densities of HNCO and residual O_3, and the rate constants for $O(^1D)$ reactions with HNCO and O_3 determined as above. This treatment indicates that a density of $O(^1D)$ + HNCO reaction products as large as 3×10^{13} cm^{-3} was produced in the photodissociation/LIF experiments. Hence, the branching fraction for production of OH + NCO by the $O(^1D)$ + HNCO reaction must be less than 0.1.

It is interesting to speculate whether a process analogous to reaction 2 occurs in the $O(^1D) + HN_3$ reaction. In that case, the products would be $NH + N_2O$, with the release of 75 kcal mol^{-1}. This exothermicity is insufficient for population of the $NH(A^3\Pi)$ state. Hence, the NH $A \rightarrow X$ emission observed in the O_3/HN_3 system is likely due to the well-known[13] dissociation of HN_3 in collisions with $N_2(A^3\Sigma_u^+)$ metastables, as previously suggested.[1]

Acknowledgment. This work was supported by the University of California, Los Alamos National Laboratory, under Subcontract 9-X2H-1467G-1.

(11) Gelernt, B.; Filseth, S. V.; Carrington, T. *Chem. Phys. Lett.* **1975**, *36*, 235.
(12) Charlton, T. R.; Okamura, T.; Thrush, B. A. *Chem. Phys. Lett.* **1982**, *89*, 98.
(13) Stedman, D. H.; Setser, D. W. *Chem. Phys. Lett.* **1968**, *2*, 542.

FEATURE ARTICLE

The Physicochemical Properties of Self-Assembled Surfactant Aggregates As Determined by Some Molecular Spectroscopic Probe Techniques

Franz Grieser* and Calum J. Drummond†

Department of Physical Chemistry, The University of Melbourne, Parkville, Victoria, 3052, Australia
(Received: November 23, 1987; In Final Form: May 26, 1988)

A review of many of the molecular spectroscopic probe techniques that have been used to determine the apparent microviscosity ($\bar{\eta}_{app}$), effective dielectric constant (ϵ_{eff}), electrostatic surface potential (Ψ_0), and size (N_{agg}) of self-assembled surfactant aggregates is given. The discussion is focused on micelles and unilamellar vesicles. Special emphasis has been placed on assessing the validity of the critical assumptions that are employed in converting spectroscopic probe data into physicochemical quantities. A comprehensive tabulation of N_{agg}, ϵ_{eff}, $\bar{\eta}_{app}$, and Ψ_0 values, as they pertain to micelles and unilamellar vesicles, is also presented as supplementary material.

1. Introduction

For the past three decades a considerable amount of research effort has been directed toward determining the physicochemical properties of self-assembled surfactant aggregates, especially micelles and unilamellar vesicles. Although many reasons can be cited for the widespread interest in elucidating the physicochemical properties of micelles and vesicles, there are primarily three reasons. Firstly, one can consistently and easily prepare aqueous micellar and vesicular solutions which have aggregates of colloidal dimensions with characteristic size, shape, and surface properties. Hence micellar and vesicular systems have been employed as model systems in investigations concerned with understanding colloidal physicochemical phenomena.[1,2] Secondly, the similarities between self-assembled surfactant aggregates, such as micelles and vesicles, and biological lipid membranes have not gone unnoticed. Thus, in many studies micelles and vesicles have served as rudimentary model systems for biological lipid membrane systems.[2,3] Thirdly, it has been found that micelles and vesicles can act as unique reaction media. Indeed, solubilization of reactants within self-assembled surfactant aggregates frequently leads to altered reaction rates, reaction routes, and stereochemistries.[2,3] Obviously micelles and vesicles cannot be fully exploited as reaction media until all their physicochemical properties have been ascertained.

† Present address: CSIRO, Division of Chemicals and Polymers, G.P.O. Box 4331, Melbourne, Victoria, 3001, Australia.

(1) *Physics of Amphiphiles, Micelles, Vesicles and Microemulsions*; De Giorgio, V., Corti, M., Eds.; North-Holland: Amsterdam, 1985.
(2) *Surfactants in Solution*; Mittal, K. L., Lindman, B., Eds.; Plenum: New York, 1984; Vol. 1 and 2.
(3) Fendler, J. H. *Membrane Mimetic Chemistry*; Wiley-Interscience: New York, 1982.

0022-3654/88/2092-5580$01.50/0